

Growing aridity and seasonality can drive catastrophic changes in the Amazon forest

Luciano J S Anjos ^{Corresp., 1, 2}, Peter M de Toledo ^{2, 3}

¹ Campus de Parauapebas, Universidade Federal Rural da Amazônia, Parauapebas, Pará, Brasil

² Programa de Pós-Graduação em Ciências Ambientais, Universidade Federal do Pará, Belém, Pará, Brasil

³ Centro de Ciência do Sistema Terrestre - CCST, Instituto Nacional de Pesquisas Espaciais, São José dos Campos, São Paulo, Brasil

Corresponding Author: Luciano J S Anjos

Email address: ljsanjos@gmail.com

The consolidation of a non-analogous climate shortly will likely affect the structure and functioning of Amazon, the most biodiverse terrestrial ecosystem on the planet. However, the ecological mechanisms underlying these potential events are still poorly understood. Here, we investigate the mechanism responsible for controlling the forest-savanna transition regime through an objective measure of resilience, based on the multidimensional climatic niche of ecosystems. Our results suggest that there is an alternating dominance, where forest and savanna have their respective basins of attraction. However, we note that the two stable states can coexist only in a narrow ecotonal zone of bistability. In this particular region, there is an equivalence between forest and savanna in quantitative terms and its presence indicates, in addition to a low hysteresis, a propensity for a catastrophic transition regime between forest and savanna. In this sense, we determine the critical levels of resilience that intermediate the dynamics of transition between forest and savanna through such bistable ecotonal zone. Also, we found that bistable region is strongly associated with critical climatic thresholds, mainly on the axis of the moisture availability and climatic seasonality, but with the lower effect of the average annual temperature. Thus, we can expect that if such climatic thresholds are reached, due to ongoing climate change, and forest resilience limits are exceeded; large-scale catastrophic events will suddenly be triggered. The expected effects are the erosion of Amazonian biodiversity, with the massive extinction of species, culminating in the consolidation of a stable state with simplified ecosystems, with a lower density of tree cover.

1 **Growing aridity and seasonality can drive catastrophic**
2 **changes in the Amazon forest**

3

4 Luciano J S Anjos^{1,2}, Peter Mann de Toledo^{1,3}

5 ¹ Programa de Pós-Graduação em Ciências Ambientais, Universidade Federal do Pará, Belém,
6 Pará, Brasil

7 ² Campus de Parauapebas, Universidade Federal Rural da Amazônia, Parauapebas, Pará, Brasil

8 ³ Centro de Ciência do Sistema Terrestre, Instituto Nacional de Pesquisas Espaciais, São José dos
9 Campos, São Paulo Brasil

10

11 Corresponding Author:

12 Luciano Anjos¹

13 PA 275, s/n, Parauapebas, Pará, 68515-000, Brasil

14 Email address: ljsanjos@gmail.com

15

16

17

18

19

20

21

22

23

24

25

26

27 Abstract

28 The consolidation of a non-analogous climate shortly will likely affect the structure and
29 functioning of Amazon, the most biodiverse terrestrial ecosystem on the planet. However, the
30 ecological mechanisms underlying these potential events are still poorly understood. Here, we
31 investigate the mechanism responsible for controlling the forest-savanna transition regime through
32 an objective measure of resilience, based on the multidimensional climatic niche of ecosystems.
33 Our results suggest that there is an alternating dominance, where forest and savanna have their
34 respective basins of attraction. However, we note that the two stable states can coexist only in a
35 narrow ecotonal zone of bistability. In this particular region, there is an equivalence between forest
36 and savanna in quantitative terms and its presence indicates, in addition to a low hysteresis, a
37 propensity for a catastrophic transition regime between forest and savanna. In this sense, we
38 determine the critical levels of resilience that intermediate the dynamics of transition between
39 forest and savanna through such bistable ecotonal zone. Also, we found that bistable region is
40 strongly associated with critical climatic thresholds, mainly on the axis of the moisture availability
41 and climatic seasonality, but with the lower effect of the average annual temperature. Thus, we
42 can expect that if such climatic thresholds are reached, due to ongoing climate change, and forest
43 resilience limits are exceeded; large-scale catastrophic events will suddenly be triggered. The
44 expected effects are the erosion of Amazonian biodiversity, with the massive extinction of species,
45 culminating in the consolidation of a stable state with simplified ecosystems, with a lower density
46 of tree cover.

47

48 **Keywords:** Tipping point, Resilience, Bistability, Forest-savanna transitions.

49

50 Introduction

51 Observational data indicate that the 2016 year was the warmest and driest in the Amazon
52 basin since the beginning of observations (Jiménez-Muñoz et al., 2016). In this context, El Niño
53 (ENSO) plays an essential role as a determining factor of extreme interannual climatic events in
54 the Amazon. This climate pattern, with higher temperatures and longer dry season duration, seems
55 to compose a trend for the biome, especially in its eastern to southwestern borders (Li et al., 2008b;
56 Fu et al., 2013; Jiménez-Muñoz et al., 2013). For the foreseeable future, this scenario is expected
57 to accentuate. Climate simulations predict that by the end of the 21st century the Amazon basin
58 will suffer from non-analogous conditions with little overlap with the current climate (Williams et
59 al., 2007; Malhi et al., 2009; Garcia et al., 2014).

60 Terrestrial ecosystems are known to depend on energy and moisture availability to
61 maintain their structure and functioning (Murphy & Bowman, 2012; Donoghue & Edwards, 2014;
62 Oliveras & Malhi, 2016)(Murphy & Bowman, 2012; Donoghue & Edwards, 2014; Oliveras &
63 Malhi, 2016). However, forests are not only a passive recipient of abiotic conditions (Zemp et al.,
64 2017)(Zemp et al., 2017). Amazon forest, with its immense biological richness (Mittermeier et al.,
65 2003), plays a vital role in the global climate system, integrating an intricate network of material
66 and energy feedbacks at large scales (Aragão et al., 2014; Nobre et al., 2016). Therefore, it is
67 expected that ongoing climate change, promoted mainly by the increasing rate of greenhouse gas
68 emissions to the atmosphere (IPCC, 2014), will affect the integrity and functioning of the Amazon
69 forest (Davidson et al., 2012). Such climate state will entail the commitment of a vast set of goods
70 and services provided to humans (Cardinale et al., 2012; Pecl et al., 2017).

71 However, there are still many uncertainties about how the forest will respond if there is a
72 consolidation of such changes in the climate. In this regard, in large part, is due to the non-inclusion

73 of biological mechanisms in the construction of predictive models (Urban et al., 2016). According
74 to the ecological stability theory (Scheffer et al., 2001), along with an environmental gradient, a
75 catastrophic transition regime can be triggered suddenly between stable states if a given resilience
76 threshold is reached. In this way, it is possible to identify the effects of bistability (Hirota et al.,
77 2011; Staver, Archibald & Levin, 2011). A central concept in ecological stability theory is that of
78 resilience. Resilience, in the context of complex ecological systems, can be interpreted as the
79 ability of an ecosystem to recover after suffering a disturbance (Holling, 1973; Pimm, 1984;
80 Scheffer et al., 2001; Folke et al., 2004).

81 In this study, to understand the potential responses of the Amazon forest to changes in
82 climate, we propose to investigate the ecological mechanism that controls forest-savanna transition
83 regimes and the implications for the forest ecosystem. To achieve this goal, we measured and
84 mapped the resilience of forest and savanna by modeling the multidimensional climatic niche of
85 ecosystems using high spatial resolution remote sensing data. This new approach, which integrates
86 different theoretical and methodological bodies, represents a significant advance for the
87 conservation of Amazonian biodiversity in order to will improve our predictive capacity in
88 anticipating catastrophic transitional events.

89

90 **Material & Methods**

91 Modeling the multidimensional climate niche of forest and savanna

92 The presence-absence data of the stable ecosystem states, used as input in ecological niche
93 modeling, were defined from a trimodal frequency histogram of the tree cover variable (0-100%)
94 from the MODIS (Moderate Resolution Imaging Spectroradiometer Satellite) (Townshend et al.,
95 2011). The spatial resolution of the raster is 6 km inside and covers all of South America. The

96 stable savanna state presents tree cover values between 5 and 60%, while forest presents values
97 over 60% (Hirota et al., 2011). Within this range, the steady state in question assumes the presence
98 value (1), and out is considered as absent (0). After correction of classification inaccuracies due to
99 the historical land use bias, based on a consensual basis of high-resolution vegetation classes
100 (Tuanmu & Jetz, 2014), the raster was converted to the point vector format, where each observation
101 received its geographical coordinate of longitude and latitude.

102 As bioclimatic predictors for ecological niche modeling, we used the climatic dataset CHPclim
103 (v.1.0) produced by the Climate Hazards Group's Precipitation Climatology with a spatial
104 resolution of 0.05° (~ 6 km) to describe the precipitation patterns of South America (Funk et al.,
105 2015). The temperature patterns along the continent were represented with the WorldClim
106 database (Hijmans et al., 2005) with a spatial resolution of 0.041° (~ 5 km). We have selected four
107 bioclimatic predictors related to energy availability (temperature) and humidity (precipitation),
108 which are recognized as essential factors from the ecophysiological point of view of ecosystems
109 (Lehmann et al., 2014; Oliveras & Malhi, 2016): annual cumulative precipitation (ACP); (2)
110 precipitation seasonality coefficient (PSC); (3) annual average of temperature (AAT) and (4)
111 annual range of temperature (ART).

112 To model the ecological niche of ecosystems as stable states, we used the biomod2 package
113 implemented in the R software (Thuiller et al., 2009). Niche models were calibrated using
114 presence-absence data from each ecosystem combined with the four bioclimatic predictors
115 described above. We have adopted the ensemble strategy, which emphasizes the most consensual
116 predictions among different modeling methods (Araújo & New, 2007; Franklin, 2010), thus
117 minimizing the effect of uncertainties on model prediction (Diniz-Filho et al., 2009)(Diniz-Filho
118 et al., 2009). We utilized ten different methods for build the models: Bioclim (SRE), Classification

119 Tree Analysis (CTA) (Scull, Franklin & Chadwick, 2005); Maxent (Phillips et al., 2006, 2016);
120 Random Forest (RF) (Breiman, 2001); Generalized Linear Models (GLM) (Guisan, Edwards &
121 Hastie, 2002); Generalized Additive Models (GAM) (Hastie & Tibshirani, 1986); Function
122 Discriminant Analysis (FDA) (Manel, Dias & Ormerod, 1999); Artificial Neural Networks (ANN)
123 (Manel, Dias & Ormerod, 1999); Multiple Additive Regression Splines (MARS) (Friedman, 1991).
124 For each method, we ran ten replicates with 75, and 25% partition for training and test,
125 respectively. We evaluated the quality of the models produced by the different methods with the
126 True Skill Statistics (TSS) and Receiver Operating Characteristic (ROC) metrics. The best models
127 to compose the ensemble were selected using the TSS metric that measures quality combining
128 sensitivity and specificity (Allouche, Tsoar & Kadmon, 2006). For threshold effect, only the
129 models with $TSS \geq 0.6$ were considered to compose the ensemble. The model of consensual
130 distribution was then obtained through the arithmetic mean among the best models of the different
131 methods (Diniz-Filho et al., 2010).

132

133 Spatial resilience boundary for forest and savanna

134 This study emphasizes the natural transition mechanisms between the Amazonian forest and
135 adjacent savanna ecosystems (e.g., cerrado) from a resilience gradient based on the
136 multidimensional climatic niche of steady states. Therefore, the study area comprises the entire
137 Amazon basin and the adjacent regions bordering the biome, located between latitudes 10 °N and
138 20 °S and longitudes 40 ° W and 80 °W. The spatial resolution of the raster is 0.05 ° (~ 6 km)
139 containing 432,042 pixels.

140 Here, climate suitability models derived from ecological niche modeling are used alternatively as
141 a direct and objective measure of ecosystem resilience. To identify the geographical limits of

142 resilience between the Amazon forest and adjacent savannas, we calculated the amplitude between
143 the resilience gradients of the two stable states over all the pixels in the study area to identify the
144 dominance zones and those where there is bistability in spatially explicit ways. Regions with high
145 amplitude values indicate that forest or savanna, depending on the area, dominate regarding
146 resilience, while low amplitude values (close to zero) suggest that there is a counterbalance of the
147 resilience between the two ecosystems, ecosystems would be equivalent to having bistability.

148

149 Predicting resilience thresholds in transition regimes

150 To identify critical resilience thresholds before forest-savanna transition regimes, we calculated
151 the observed proportion of each stable state (forest or savanna) along each measured unit of forest
152 resilience to the study area. We counted a total of 446 independent and non-autocorrelated samples,
153 where the forest and savanna ratio were calculated, ranging from 0 (zero) to 1 (one) along the
154 resilience gradient. The observed proportions, such as response variable, were then plotted as a
155 function of the forest resilience gradient. Then, we fitted a non-linear local regression statistical
156 model (LOESS) to the observed data to estimate the critical cut points under the resilience gradient
157 at the moment the curves assumed independent behavior and diverged each other.

158

159 Calculating the trend towards a transition regime and its associated climatic thresholds

160 We measured the propensity for transitions regimes from the spatial anomaly of resilience
161 calculation between the rasters of the two stable states. The values of the output of the operation
162 vary between [+1000] (positive), which are related to the increase of the forest resilience, and [-
163 1000] (negative) indicating an increase of the resilience of savanna. Using this gradient, we
164 counted the number of forest and savanna observations under each unit of the measured anomaly

165 to calculate the observed proportion of forest and savanna along the gradient of the anomaly. After
166 this procedure, which generated a set of 1,805 observations with statistical independence and
167 without spatial autocorrelation, we plot the observations under a two-dimensional scatterplot,
168 where the respective bioclimatic predictors are the axes.

169 We separate the factors under the two-dimensional climate space in (a) energy availability and
170 humidity and (b) climatic seasonality. After this, we then fit a linear model, which the orientation
171 of the line will indicate the type of statistical relationship between the predictors and the tendency
172 to transformations between the ecosystems. By assigning a color gradient, related to the trend
173 variable to a transition regime, it was also possible to identify the climatic thresholds critical to the
174 transition between stable states from abrupt color changes.

175

176 **Results**

177 We map the distribution of ecosystem resilience of stable forest and savanna states based on the
178 occupation of their respective multidimensional climatic niches (Figure 1A and B). The models
179 presented high sensitivity in predicting the alternating dominance of stable states over space with
180 synchronized geographic substitution between ecosystems. Such pattern of alternating dominance
181 between the two stable states is further evident in Figure 1C, where high resilience amplitude
182 values dominate almost the entire study area. However, we have detected only a narrow boundary
183 of bistability between the two ecosystems, where low values of resilience amplitude (close to zero)
184 prevail, highlighted by the black rectangles in Figure 1C. Such a bistable ecotonal zone should be
185 responsible for the mediation of transition events between the two stable states, being described in
186 the theoretical field as Maxwell's point. Its presence indicates, in addition to bistability among the
187 ecosystems, a low hysteresis, in case the return to the original stable state occurs.

188 Figure 1. Ecosystem resilience gradient and Maxwell point detection. Estimated climate resilience
189 for the forest (A) and savanna (B). In (C), the amplitude of resilience between forest and savanna
190 gradients. The rectangles in (C) under the lowest values indicate the boundary between the two
191 ecosystems, where a bistability pattern and low hysteresis prevail.

192

193 In Figure 2, we observed empirically, under the forest resilience gradient, that, from a given
194 boundary, towards the highest values, there is a predominance of the stable state of forest (green
195 balls), reflected in the highest proportion of observations when compared to savannas (purple
196 balls). Below an absolute limit of resilience, toward the lower values, the pattern reverses, since
197 there is proportionately more savanna than forest. However, between the two extremes of the
198 gradient, we identified an ecotonal resilience zone (green-moss rectangle), where the observed
199 values between forest and savanna are proportionally similar (~ 0.5). Such pattern indicates the
200 presence of mosaics of habitats in the landscape, where there is a dominance of either of the two
201 stable states (Figure 2). With the aid of a non-linear local regression model fitted to the data, we
202 observed that critical resilience values before catastrophic transition events between forest and
203 savanna are between 704 to 448 under the forest resilience gradient.

204

205 Figure 2. Critical resilience thresholds and the bistable ecotonal zone. Under high resilience values
206 (≥ 704) dominance of forests (green balls), while in low values (≤ 448) savannas stand out
207 (purple balls). Under an intermediate zone of the resilience gradient (green-moss polygon), there
208 is a balance of the observed proportions of forest and savanna, indicating an area of bistability.
209 This transition zone should play a vital role in the mediation of stable state change events between
210 forest and savanna.

211 In Figure 3, we present a trend metric for catastrophic transition regimes under the two-
212 dimensional climate space of the study area. In the graph of energy availability and humidity for
213 ecosystems (Figure 3A), we observed that there is a strong tendency towards catastrophic
214 transformations between forest and savanna associated with a critical threshold of moisture
215 availability. At precipitation levels below the threshold of 1500 mm/year (ACP), there is a sudden
216 change with an evident increase in the chance to savanna, independent of the observed mean annual
217 temperature (AAT) values. On the other hand, in the climatic seasonality graph (Figure 3B), the
218 results indicate that the increase in climatic seasonality, both regarding temperature (ART) and
219 precipitation (PSC), are positively correlated with the tendency to more open environments in the
220 area of study. Such pattern may lead to events of sudden transitions from forest to savanna.

221

222 Figure 3. The propensity for catastrophic transition regimes under bidimensional climate space. In
223 (A) on the X-axis is the average annual temperature gradient (AAT) and on the Y-axis the annual
224 cumulative precipitation (ACP). In (B) on the X-axis is the annual range of temperature (ART)
225 and on the Y-axis is the seasonal precipitation coefficient (PSC). In all, we used $n=1805$
226 observations.

227

228 Discussion

229 The evidence presented here, such as Maxwell's point detection in a spatially explicit way,
230 reinforces that a possible transition regime between forest and savanna would occur suddenly and
231 in catastrophic proportions, if the critical resilience threshold is reached (Staal et al., 2016). The
232 erosion of biodiversity, with the massive extinction of forest species through a phenomenon
233 described as die-back forest (Cox et al., 2004), would result in the systematic loss of resilience

234 induced by anthropogenic environmental changes. This process of degradation, in theory, would
235 culminate in the consolidation of another level of ecological stability on the Amazon basin, with a
236 lower density of tree cover (e.g., savannas) (Zemp et al., 2017). This result is possible because
237 forests are more vulnerable to climate change shortly than other terrestrial ecosystems (Perez,
238 Stroud & Feeley, 2016).

239 It appears that the transition process over the Amazon basin has already begun (Malhi et al., 2008;
240 Davidson et al., 2012). Observed empirical evidence, with data from different sources, has shown
241 that the forest is losing its natural self-regeneration capacity. In general, slower recovery of these
242 ecosystems has been observed in structural and functional terms after disturbances, mainly under
243 the southeastern and eastern edges of the biome, near the ecotonal zone with the cerrado. For
244 example, the ability of forests to retain carbon in biomass in this region has been compromised as
245 a function of the observed moisture deficit (Phillips et al., 2009; Brienen et al., 2015; Feldpausch
246 et al., 2016; Baccini et al., 2017). Amazonian floodplain forests have also shown a slower recovery
247 rate after fire events and prolonged dry periods (Flores et al., 2017). In the same sense, severe
248 drought events are also associated with high tree mortality rates (Allen et al., 2010; Greenwood et
249 al., 2017), with effects aggravated by forest fires (Barlow & Peres, 2008; Brando et al., 2014).

250 In this sense, the explicit determination of critical thresholds of resilience at large scales means a
251 particularly significant advance for Amazonian conservation, since we would have a better
252 predictive capacity to anticipate the effects of climate changes on the forest. Such information will
253 guarantee a more precise action towards ecosystem conservation plans (Scheffer et al., 2015).

254 Some authors have already explored this hypothesis previously based on coupled models of
255 climate and vegetation dynamics (Oyama & Nobre, 2003; Nobre & Borma, 2009; Salazar &

256 Nobre, 2010), but without explicitly exploring the ecological mechanism underlying transition
257 regimes.

258 The bistable ecotonal zone (Maxwell point) is associated with catastrophic transition regimes and
259 also indicates the presence of an environmentally well-defined threshold (Wuyts, Champneys &
260 House, 2017). In this sense, the correlation of the observed trends to a transition regime under the
261 two-dimensional climate space allowed the design of a useful climatic metric, which indicates the
262 thresholds for the monitoring of catastrophic events. Also, with such a procedure it was possible
263 to measure the importance of bioclimatic predictors in determining potential devastating transition
264 regimes.

265 Our findings indicate that changes in mean temperature would have little influence on the
266 transition regime between forest and savanna. In other words, with a higher concentration of
267 greenhouse and increasing global temperatures, will not be the primary factor that will determine
268 catastrophic transition events between forest and savanna. Although the relevance of the effect of
269 CO₂ fertilization on forest productivity is recognized (Lloyd & Farquhar, 2008; Cox et al., 2013;
270 Huntingford et al., 2013).

271 Our results indicate that the most important factor when analyzing the energy and humidity
272 availability axis is the annual cumulative volume of precipitation. According to our findings, in
273 order not to trigger catastrophic transition events between forest and savanna, it would have to rain
274 at least 1500 mm/year in a particular region. Some authors corroborate this critical climatic
275 threshold with other methodological approaches (Malhi et al., 2009; Wuyts, Champneys & House,
276 2017). In a recent study, the author indicates a breakpoint of approximately 2000 mm/year
277 (Ahlström et al., 2017) as a critical value for the maintenance of high values of gross primary
278 productivity. Although, the conclusion was not based on an objective measure of ecosystem

279 resilience. However, all the data observed and simulated indicate a tendency to increase aridity
280 over the Amazon basin (Li et al., 2008a; Malhi et al., 2009; Fu et al., 2013; Boisier et al., 2015;
281 Erfanian, Wang & Fomenko, 2017), specially on the southwest and east edges of the biome.
282 Under the climatic seasonality, our results indicate that the increase in seasonality of precipitation
283 and temperature has a direct association with a higher propensity for catastrophic transition
284 regimes between forest and savanna. These data suggest that rainfall is more frequent in the
285 Amazon basin due to the prolongation of the dry season, mainly on the eastern edges of the
286 southwest (Li et al., 2008a; Fu et al., 2013; Boisier et al., 2015). Another negative factor, which
287 has further accentuated the increasing seasonality of precipitation, is the increase in the frequency
288 of extreme drought events, mainly caused by more severe El-Niño (Jiménez-Muñoz et al., 2016).
289 Our results indicate that, as a function of the alternating dominance pattern through the resilience
290 gradient, the Amazonian forest and adjacent savanna ecosystems represent two independent stable
291 states, where each one has its basin of attraction, previous corroborating studies (Hirota et al.,
292 2011; Staver, Archibald & Levin, 2011). However, our findings suggest that coexistence between
293 savanna and forest is restricted to a narrow ecotonal zone of best ability, known as Maxwell's
294 point, contrary to the hypothesis that forests and savannas have extensive areas of bimodality
295 (Staver, Archibald & Levin, 2011). Such pattern can be explained by the fact that our models were
296 based on the multidimensional climatic niche of stable states, which means a higher sensitivity due
297 to better ecological resolution when compared to previous, generally two-dimensional, studies.
298 Wuyts et al. (2017) found a similar result to this study, also indicating that human activities, such
299 as changes in soil use, have promoted the increase of bistability in the tropical region of South
300 America.
301

302 Conclusions

303 The loss of resilience due to climate change can lead to sudden catastrophic transition events
304 between forest and savanna in the tropical region. Reducing the availability of moisture and
305 increasing climatic seasonality appear as the main risk factors. If such critical climatic thresholds
306 are reached, there will probably be the massive extinction of biodiversity in the Amazon rainforest.

307

308 Acknowledgments

309 We are grateful to Ima Celia Guimaraes Vieira, Aline Meiguins de Lima, Roberta Macedo
310 Cerqueira and Edson Jose Paulino da Rocha for their valuable contributions and suggestions
311 throughout the development of this work.

312

313 References

314 Ahlström A., Canadell JG., Schurgers G., Wu M., Berry JA., Guan K., Jackson RB. 2017.
315 Hydrologic resilience and Amazon productivity. *Nature Communications* 8:387. DOI:
316 10.1038/s41467-017-00306-z.

317 Allen CD., Macalady AK., Chenchouni H., Bachelet D., McDowell N., Vennetier M., Kitzberger
318 T., Rigling A., Breshears DD., Hogg EH (Ted), Gonzalez P., Fensham R., Zhang Z., Castro J.,
319 Demidova N., Lim JH., Allard G., Running SW., Semerci A., Cobb N. 2010. A global overview
320 of drought and heat-induced tree mortality reveals emerging climate change risks for forests.
321 *Forest Ecology and Management* 259:660–684. DOI: 10.1016/j.foreco.2009.09.001.

322 Allouche O., Tsoar A., Kadmon R. 2006. Assessing the accuracy of species distribution models:
323 Prevalence, kappa and the true skill statistic (TSS). *Journal of Applied Ecology* 43:1223–1232.
324 DOI: 10.1111/j.1365-2664.2006.01214.x.

325 Aragão LEOC., Poulter B., Barlow JB., Anderson LO., Malhi Y., Saatchi S., Phillips OL., Gloor
326 E. 2014. Environmental change and the carbon balance of Amazonian forests. *Biological Reviews*
327 89:913–931. DOI: 10.1111/brv.12088.

328 Araújo MB., New M. 2007. Ensemble forecasting of species distributions. *Trends in Ecology and*
329 *Evolution* 22:42–47. DOI: 10.1016/j.tree.2006.09.010.

330 Baccini A., Walker W., Carvahlo L., Farina M., Sulla-Menashe D., Houghton R. 2017. Tropical
331 forests are a net carbon source based on new measurements of gain and loss. *In review* 5962:1–11.

- 332 DOI: 10.1126/science.1252826.
- 333 Barlow J., Peres CA. 2008. Fire-mediated dieback and compositional cascade in an Amazonian
334 forest. *Philosophical transactions of the Royal Society of London. Series B, Biological sciences*
335 363:1787–1794. DOI: 10.1098/rstb.2007.0013.
- 336 Boisier JP., Ciais P., Ducharne A., Guimberteau M. 2015. Projected strengthening of Amazonian
337 dry season by constrained climate model simulations. *Nature Climate Change* 5:656–660. DOI:
338 10.1038/nclimate2658.
- 339 Brando PM., Balch JK., Nepstad DC., Morton DC., Putz FE., Coe MT., Silvério D., Macedo MN.,
340 Davidson E a., Nóbrega CC., Alencar A., Soares-Filho BS. 2014. Abrupt increases in Amazonian
341 tree mortality due to drought-fire interactions. *Proceedings of the National Academy of Sciences*
342 *of the United States of America* 111:6347–52. DOI: 10.1073/pnas.1305499111.
- 343 Brienen RJW., Phillips OL., Feldpausch TR., Gloor E., Baker TR., Lloyd J., Lopez-Gonzalez G.,
344 Monteagudo-Mendoza A., Malhi Y., Lewis SL., Vásquez Martínez R., Alexiades M., Álvarez
345 Dávila E., Alvarez-Loayza P., Andrade A., Aragão LEOC., Araujo-Murakami A., Arets EJMM.,
346 Arroyo L., Aymard C GA., Bánki OS., Baraloto C., Barroso J., Bonal D., Boot RGA., Camargo
347 JLC., Castilho C V., Chama V., Chao KJ., Chave J., Comiskey JA., Cornejo Valverde F., da Costa
348 L., de Oliveira EA., Di Fiore A., Erwin TL., Fauset S., Forsthofer M., Galbraith DR., Grahame
349 ES., Groot N., Hérault B., Higuchi N., Honorio Coronado EN., Keeling H., Killeen TJ., Laurance
350 WF., Laurance S., Licona J., Magnussen WE., Marimon BS., Marimon-Junior BH., Mendoza C.,
351 Neill DA., Nogueira EM., Núñez P., Pallqui Camacho NC., Parada A., Pardo-Molina G., Peacock
352 J., Peña-Claros M., Pickavance GC., Pitman NCA., Poorter L., Prieto A., Quesada CA., Ramírez
353 F., Ramírez-Angulo H., Restrepo Z., Roopsind A., Rudas A., Salomão RP., Schwarz M., Silva N.,
354 Silva-Espejo JE., Silveira M., Stropp J., Talbot J., ter Steege H., Teran-Aguilar J., Terborgh J.,
355 Thomas-Caesar R., Toledo M., Torello-Raventos M., Umetsu RK., van der Heijden GMF., van
356 der Hout P., Guimarães Vieira IC., Vieira SA., Vilanova E., Vos VA., Zagt RJ. 2015. Long-term
357 decline of the Amazon carbon sink. *Nature* 519:344–8. DOI: 10.1038/nature14283.
- 358 Cardinale BJ., Duffy JE., Gonzalez A., Hooper DU., Perrings C., Venail P., Narwani A., Mace
359 GM., Tilman D., A. Wardle D., Kinzig AP., Daily GC., Loreau M., Grace JB., Larigauderie A.,
360 Srivastava DS., Naeem S. 2012. Biodiversity loss and its impact on humanity. *Nature* 489:326–
361 326. DOI: 10.1038/nature11373.
- 362 Cox PM., Betts RA., Collins M., Harris PP., Huntingford C., Jones CD. 2004. Amazonian forest
363 dieback under climate-carbon cycle projections for the 21st century. *Theoretical and Applied*
364 *Climatology* 78:137–156. DOI: 10.1007/s00704-004-0049-4.
- 365 Cox PM., Pearson D., Booth BB., Friedlingstein P., Huntingford C., Jones CD., Luke CM. 2013.
366 Sensitivity of tropical carbon to climate change constrained by carbon dioxide variability. *Nature*
367 494:341–344. DOI: 10.1038/nature11882.
- 368 Davidson EA., de Araújo AC., Artaxo P., Balch JK., Brown IF., C Bustamante MM., Coe MT.,
369 DeFries RS., Keller M., Longo M., Munger JW., Schroeder W., Soares-Filho BS., Souza CM.,
370 Wofsy SC., C. Bustamante MM., Coe MT., DeFries RS., Keller M., Longo M., Munger JW.,
371 Schroeder W., Soares-Filho BS., Souza CM., Wofsy SC., Bustamante MMC., Arau AC De., Coe

- 372 MT., DeFries RS., Keller M., Longo M., Munger JW., Schroeder W., de Araújo AC., Artaxo P.,
373 Balch JK., Brown IF., C Bustamante MM., Coe MT., DeFries RS., Keller M., Longo M., Munger
374 JW., Schroeder W., Soares-Filho BS., Souza CM., Wofsy SC., C. Bustamante MM., Coe MT.,
375 DeFries RS., Keller M., Longo M., Munger JW., Schroeder W., Soares-Filho BS., Souza CM.,
376 Wofsy SC. 2012. The Amazon basin in transition. *Nature* 481:321–328. DOI:
377 10.1038/nature10717.
- 378 Diniz-Filho JAF., Bini LM., Rangel TF., Loyola RD., Hof C., Nogue D., Arau MB., Diniz-Filho
379 JAF., Mauricio Bini L., Fernando Rangel T., Loyola RD., Hof C., Noguã@s-Bravo D., Araã°jo
380 MB. 2009. Partitioning and mapping uncertainties in ensembles of forecasts of species turnover
381 under climate change. *Ecography* 32:897–906. DOI: 10.1111/j.1600-0587.2009.06196.x.
- 382 Diniz-Filho JAF., Ferro VG., Santos T., Nabout JC., Dobrovolski R., De Marco P. 2010. The three
383 phases of the ensemble forecasting of niche models : geographic range and shifts in climatically
384 suitable areas of *Utetheisa ornatrix*. *Revista Brasileira de Entomologia* 54:339–349.
- 385 Donoghue MJ., Edwards EJ. 2014. Biome Shifts and Niche Evolution in Plants. *Annual Review of*
386 *Ecology, Evolution, and Systematics* 45:547–572. DOI: 10.1146/annurev-ecolsys-120213-091905.
- 387 Erfanian A., Wang G., Fomenko L. 2017. Unprecedented drought over tropical South America in
388 2016: significantly under-predicted by tropical SST. *Scientific Reports* 7:5811. DOI:
389 10.1038/s41598-017-05373-2.
- 390 Feldpausch TR., Phillips OL., Brienen RJW., Gloor E., Lloyd J., Malhi Y., Alarcón A., Dávila
391 EÁ., Andrade A., Aragao LEOC., Arroyo L., Aymard GAC., Baker TR., Baraloto C., Barroso J.,
392 Bonal D., Castro W., Chama V., Chave J., Domingues TF., Fauset S., Groot N., Coronado EH.,
393 Laurance S., Laurance WF., Lewis SL., Licona JC., Marimon BS., Bautista CM., Neill DA.,
394 Oliveira EA., Santos CO., Camacho NCP., Prieto A., Quesada CA., Ramírez F., Rudas A., Saiz
395 G., Salomão RP., Silveira M., Steege H., Stropp J., Terborgh J., Heijden GMF., Martinez RV.,
396 Vilanova E., Vos VA. 2016. Amazon forest response to repeated droughts. *Global Biogeochemical*
397 *Cycles* 30:964–982. DOI: 10.1002/2015GB005133. Received.
- 398 Flores BM., Holmgren M., Xu C., van Nes EH., Jakovac CC., Mesquita RCG., Scheffer M. 2017.
399 Floodplains as an Achilles' heel of Amazonian forest resilience. *Proceedings of the National*
400 *Academy of Sciences*:201617988. DOI: 10.1073/pnas.1617988114.
- 401 Folke C., Carpenter S., BrianWalker., Scheffer M., Elmqvist T., Gunderson L., Holling CSS.,
402 Walker B., Scheffer M., Elmqvist T., Gunderson L., Holling CSS. 2004. Regime Shifts, Resilience,
403 and Biodiversity in Ecosystem Management. *Annual Review of Ecology, Evolution, and*
404 *Systematics* 35:557–581. DOI: 10.1146/annurev.ecolsys.35.021103.105711.
- 405 Franklin J. 2010. Mapping species distributions: spatial inference and prediction.
- 406 Friedman JH. 1991. Multivariate Adaptive Regression Splines. *The Annals of Statistics* 19:1–67.
407 DOI: 10.1214/aos/1176347963.
- 408 Fu R., Yin L., Li W., Arias PA., Dickinson RE., Huang L., Chakraborty S., Fernandes K.,
409 Liebmann B., Fisher R., Myneni RB. 2013. Increased dry-season length over southern Amazonia

- 410 in recent decades and its implication for future climate projection. *Proceedings of the National*
411 *Academy of Sciences* 110:18110–18115. DOI: 10.1073/pnas.1302584110.
- 412 Funk C., Verdin A., Michaelsen J., Peterson P., Pedreros D., Husak G. 2015. A global satellite-
413 assisted precipitation climatology. *Earth System Science Data* 7:1–15. DOI: 10.5676/DWD.
- 414 Garcia RA., Cabeza M., Rahbek C., Araujo MB. 2014. Multiple Dimensions of Climate Change
415 and Their Implications for Biodiversity. *Science* 344:1247579–1247579. DOI:
416 10.1126/science.1247579.
- 417 Greenwood S., Ruiz-Benito P., Martínez-Vilalta J., Lloret F., Kitzberger T., Allen CD., Fensham
418 R., Laughlin DC., Kattge J., Bönisch G., Kraft NJB., Jump AS. 2017. Tree mortality across biomes
419 is promoted by drought intensity, lower wood density and higher specific leaf area. *Ecology*
420 *Letters*. DOI: 10.1111/ele.12748.
- 421 Guisan A., Edwards TC., Hastie T. 2002. Generalized linear and generalized additive models in
422 studies of species distributions : setting the scene. *Ecological Modelling* 157.
- 423 Hastie T., Tibshirani R. 1986. Generalized Additive Models. *Statistics* 10:409–435. DOI:
424 10.1214/ss/1177013604.
- 425 Hijmans RJ., Cameron SE., Parra JL., Jones PG., Jarvis A. 2005. Very high resolution interpolated
426 climate surfaces for global land areas. *International Journal of Climatology* 25:1965–1978. DOI:
427 10.1002/joc.1276.
- 428 Hirota M., Holmgren M., Nes EH Van., Scheffer M. 2011. Global Resilience of Tropical Forest
429 and Savanna to Critical Transitions. *Science* 334:232–235. DOI: 10.1126/science.1210657.
- 430 Holling CS. 1973. Resilience and Stability of Ecological Systems. *Annual Review of Ecology and*
431 *Systematics* 4:1–23. DOI: 10.1146/annurev.es.04.110173.000245.
- 432 Huntingford C., Zelazowski P., Galbraith D., Mercado LM., Sitch S., Fisher R., Lomas M., Walker
433 AP., Jones CD., Booth BBB., Malhi Y., Hemming D., Kay G., Good P., Lewis SL., Phillips OL.,
434 Atkin OK., Lloyd J., Gloor E., Zaragoza-Castells J., Meir P., Betts R., Harris PP., Nobre C.,
435 Marengo J., Cox PM. 2013. Simulated resilience of tropical rainforests to CO₂-induced climate
436 change. *Nature Geoscience* 6:268–273. DOI: 10.1038/ngeo1741.
- 437 IPCC. 2014. Climate Change 2014 Synthesis Report. *Contribution of Working Groups I, II and III*
438 *to the Fifth Assessment Report of the Intergovernmental Panel on Climate Change*:1–151.
- 439 Jiménez-Muñoz JC., Mattar C., Barichivich J., Santamaría-Artigas A., Takahashi K., Malhi Y.,
440 Sobrino JA., Schrier G van der. 2016. Record-breaking warming and extreme drought in the
441 Amazon rainforest during the course of El Niño 2015–2016. *Scientific Reports* 6:33130. DOI:
442 10.1038/srep33130.
- 443 Jiménez-Muñoz JC., Sobrino JA., Mattar C., Malhi Y. 2013. Spatial and temporal patterns of the
444 recent warming of the Amazon forest. *Journal of Geophysical Research Atmospheres* 118:5204–
445 5215. DOI: 10.1002/jgrd.50456.

- 446 Lehmann CER., Anderson TM., Sankaran M., Higgins SI., Archibald S., Hoffmann WA., Hanan
447 NP., Williams RJ., Fensham RJ., Felfili J., Hutley LB., Ratnam J., Jose JS., Montes R., Franklin
448 D., Russell-Smith J., Ryan CM., Durigan G., Hiernaux P., Haidar R., Bowman DMJS., Bond WJ.,
449 San Jose J., Montes R., Franklin D., Russell-Smith J., Ryan CM., Durigan G., Hiernaux P., Haidar
450 R., Bowman DMJS., Bond WJ. 2014. Savanna Vegetation-Fire-Climate Relationships Differ
451 Among Continents. *Science* 343:548–553. DOI: 10.1126/science.1247355.
- 452 Li W., Fu R., Juarez RIN., Fernandes K. 2008a. Observed change of the standardized precipitation
453 index, its potential cause and implications to future climate change in the Amazon region.
454 *Philosophical Transactions of the Royal Society B: Biological Sciences* 363:1767–1772. DOI:
455 10.1098/rstb.2007.0022.
- 456 Li W., Fu R., Juarez RIN., Fernandes K., Juárez RIN., Fernandes K. 2008b. Observed change of
457 the standardized precipitation index, its potential cause and implications to future climate change
458 in the Amazon region. *Philosophical transactions of the Royal Society of London. Series B,*
459 *Biological sciences* 363:1767–72. DOI: 10.1098/rstb.2007.0022.
- 460 Lloyd J., Farquhar GD. 2008. Effects of rising temperatures and [CO₂] on the physiology of
461 tropical forest trees. *Philosophical Transactions of the Royal Society B: Biological Sciences*
462 363:1811–1817. DOI: 10.1098/rstb.2007.0032.
- 463 Malhi Y., Aragao LEOC., Galbraith D., Huntingford C., Fisher R., Zelazowski P., Sitch S.,
464 McSweeney C., Meir P. 2009. Exploring the likelihood and mechanism of a climate-change-
465 induced dieback of the Amazon rainforest. *Proceedings of the National Academy of Sciences*
466 106:20610–20615. DOI: 10.1073/pnas.0804619106.
- 467 Malhi Y., Roberts JT., Betts RA., Killeen TJ., Li W., Nobre CA. 2008. Climate change,
468 deforestation, and the fate of the Amazon. *Science (New York, N.Y.)* 319:169–72. DOI:
469 10.1126/science.1146961.
- 470 Manel S., Dias JM., Ormerod SJ. 1999. Comparing discriminant analysis, neural networks and
471 logistic regression for predicting species distributions: A case study with a Himalayan river bird.
472 *Ecological Modelling* 120:337–347. DOI: 10.1016/S0304-3800(99)00113-1.
- 473 Mittermeier R a., Mittermeier CG., Brooks TM., Pilgrim JD., Konstant WR., Fonseca GAB.,
474 Kormos C., da Fonseca G a B., Kormos C., Fonseca GAB., Kormos C., da Fonseca G a B., Kormos
475 C. 2003. Wilderness and biodiversity conservation. *Proceedings of the National Academy of*
476 *Sciences of the United States of America* 100:10309–13. DOI: 10.1073/pnas.1732458100.
- 477 Murphy BP., Bowman DMJS. 2012. What controls the distribution of tropical forest and savanna?
478 *Ecology Letters* 15:748–758. DOI: 10.1111/j.1461-0248.2012.01771.x.
- 479 Nobre CA., Borma LDS. 2009. “Tipping points” for the Amazon forest. *Current Opinion in*
480 *Environmental Sustainability* 1:28–36. DOI: 10.1016/j.cosust.2009.07.003.
- 481 Nobre CA., Sampaio G., Borma LS., Castilla-Rubio JC., Silva JS., Cardoso M. 2016. Land-use
482 and climate change risks in the Amazon and the need of a novel sustainable development paradigm.
483 *Proceedings of the National Academy of Sciences of the United States of America* 113:10759–

- 484 10768. DOI: 10.1073/pnas.1605516113.
- 485 Oliveras I., Malhi Y. 2016. Many shades of green: The dynamic tropical forest-savanna transitions.
486 *Philosophical Transactions. Series B, Biological Sciences*. DOI: 10.1002/cjoc.2013xxxxx.
- 487 Oyama MD., Nobre CA. 2003. A new climate-vegetation equilibrium state for Tropical South
488 America. 30:10–13. DOI: 10.1029/2003GL018600.
- 489 Pecl GT., Araujo MB., Bell JD., Blanchard J., Bonebrake TC., Chen I-C., Clark T., Colwell RK.,
490 Danielsen F., Evengard B., Falconi L., Ferrier S., Frusher S., Garcia RA., Griffis RB., Hobday AJ.,
491 Janion-Scheepers C., Jarzyna MA., Jennings S., Lenoir J., Linnetved HI., Martin VY., McCormack
492 PC., McDonald J., Mitchel NJ. 2017. Biodiversity redistribution under climate change: impacts on
493 ecosystems and human well-being. *Science* in press. DOI: 10.1126/science.aai9214.
- 494 Perez TM., Stroud JT., Feeley KJ. 2016. Thermal trouble in the tropics. *Science* 351:1392–1393.
495 DOI: 10.1126/science.aaf3343.
- 496 Phillips SJ., Anderson RP., Dudík M., Schapire RE., Blair ME. 2016. Opening the black box: an
497 open-source release of Maxent. *Ecography* 40:887–893. DOI: 10.1111/ecog.03049.
- 498 Phillips SJ., Anderson RP., Schapire RE., Phillips ENCANDPR., J S., Anderson RP., Schapire
499 RE. 2006. Maximum entropy modeling of species geographic distributions. *Ecol. Modell* 190:231–
500 259. DOI: 10.1016/j.ecolmodel.2005.03.026.
- 501 Phillips OL., Aragão LEOC., Lewis SL., Fisher JB., Lloyd J., López-González G., Malhi Y.,
502 Monteagudo A., Peacock J., Quesada C a., van der Heijden G., Almeida S., Amaral I., Arroyo L.,
503 Aymard G., Baker TR., Bánki O., Blanc L., Bonal D., Brando P., Chave J., de Oliveira ACA.,
504 Cardozo ND., Czimczik CI., Feldpausch TR., Freitas MA., Gloor E., Higuchi N., Jiménez E.,
505 Lloyd G., Meir P., Mendoza C., Morel A., Neill D a., Nepstad D., Patiño S., Peñuela MC., Prieto
506 A., Ramírez F., Schwarz M., Silva J., Silveira M., Thomas AS., Steege H Ter., Stropp J., Vásquez
507 R., Zelazowski P., Alvarez Dávila E., Andelman S., Andrade A., Chao K., Erwin T., Di Fiore A.,
508 Honorio C E., Keeling H., Killeen TJ., Laurance WF., Peña Cruz A., Pitman NC a., Núñez Vargas
509 P., Ramírez-Angulo H., Rudas A., Salamão R., Silva N., Terborgh J., Torres-Lezama A., Heijden
510 G Van Der., Cristina Á., Oliveira A De., Dávila EA., Fiore A Di., C EH., Cruz AP., Vargas PN.
511 2009. Drought Sensitivity of the Amazon Rainforest. *Science* 323:1344–1347. DOI:
512 10.1126/science.1164033.
- 513 Pimm SL. 1984. The complexity and stability of ecosystems. *Nature* 307:321–326. DOI:
514 10.1038/315635c0.
- 515 Salazar LF., Nobre CA. 2010. Climate change and thresholds of biome shifts in Amazonia.
516 *Geophysical Research Letters* 37:1–5. DOI: 10.1029/2010GL043538.
- 517 Scheffer M., Barrett S., Carpenter SR., Folke C., Green AJ., Holmgren M., Hughes TP., Kosten
518 S., Van de Leemput I a., Nepstad DC., Van Nes EH., Peeters ETHM., Walker B. 2015. Creating a
519 safe operating space for iconic ecosystems. *Science*:8–10. DOI: 10.1126/science.aaa9484.
- 520 Scheffer M., Carpenter S., Foley J a., Folke C., Walker B. 2001. Catastrophic shifts in ecosystems.

- 521 *Nature* 413:591–6. DOI: 10.1038/35098000.
- 522 Scull P., Franklin J., Chadwick OA. 2005. The application of classification tree analysis to soil
523 type prediction in a desert landscape. *Ecological Modelling* 181:1–15. DOI:
524 10.1016/j.ecolmodel.2004.06.036.
- 525 Staal A., Dekker SC., Xu C., van Nes EH. 2016. Bistability, Spatial Interaction, and the
526 Distribution of Tropical Forests and Savannas. *Ecosystems* 19:1080–1091. DOI: 10.1007/s10021-
527 016-0011-1.
- 528 Staver AC., Archibald S., Levin S. 2011. The Global Extent and Determinants of Savanna and
529 Forest as Alternative Biome States. *Science* 334:230–232. DOI: 10.1126/science.1210465.
- 530 Thuiller W., Lafourcade B., Engler R., Araújo MB., Araujo MB. 2009. BIOMOD - a platform for
531 ensemble forecasting of species distributions. *Ecography* 32:369–373. DOI: 10.1111/j.1600-
532 0587.2008.05742.x.
- 533 Townshend JR., Hansen MC., Carroll M., DiMiceli C., Sohlberg R., Huang C. 2011. Vegetation
534 Continuous Fields MOD44B, 2010 Percent Tree Cover. *Collection 5, University of Maryland,*
535 *College Park, Maryland*:1–12. DOI: <http://glsf.umiacs.umd.edu/data/vcf/>.
- 536 Tuanmu MN., Jetz W. 2014. A global 1-km consensus land-cover product for biodiversity and
537 ecosystem modelling. *Global Ecology and Biogeography* 23:1031–1045. DOI:
538 10.1111/geb.12182.
- 539 Urban MC., Bocedi G., Hendry AP., Mihoub J-B., Peer G., Singer A., Bridle JR., Crozier LG., De
540 Meester L., Godsoe W., Gonzalez A., Hellmann JJ., Holt RD., Huth A., Johst K., Krug CB.,
541 Leadley PW., Palmer SCF., Pantel JH., Schmitz A., Zollner PA., Travis JMJ. 2016. Improving the
542 forecast for biodiversity under climate change. *Science* 353:aad8466-aad8466. DOI:
543 10.1126/science.aad8466.
- 544 Williams JW., Jackson ST., Kutzbach JE. 2007. Projected distributions of novel and disappearing
545 climates by 2100 AD.
- 546 Wuyts B., Champneys AR., House JI. 2017. Amazonian forest-savanna bistability and human
547 impact. *Nature Communications* 8:15519. DOI: 10.1038/ncomms15519.
- 548 Zemp DC., Schleussner C-F., Barbosa HMJ., Hirota M., Montade V., Sampaio G., Staal A., Wang-
549 Erlandsson L., Rammig A. 2017. Self-amplified Amazon forest loss due to vegetation-atmosphere
550 feedbacks. *Nature Communications* 8:14681. DOI: 10.1038/ncomms14681.
- 551
- 552
- 553

Figure 1

Ecosystem resilience gradient and Maxwell point detection.

Estimated climate resilience for the forest (A) and savanna (B). In (C), the amplitude of resilience between forest and savanna gradients. The rectangles in (C) under the lowest values indicate the boundary between the two ecosystems, where a bistability pattern and low hysteresis prevail.

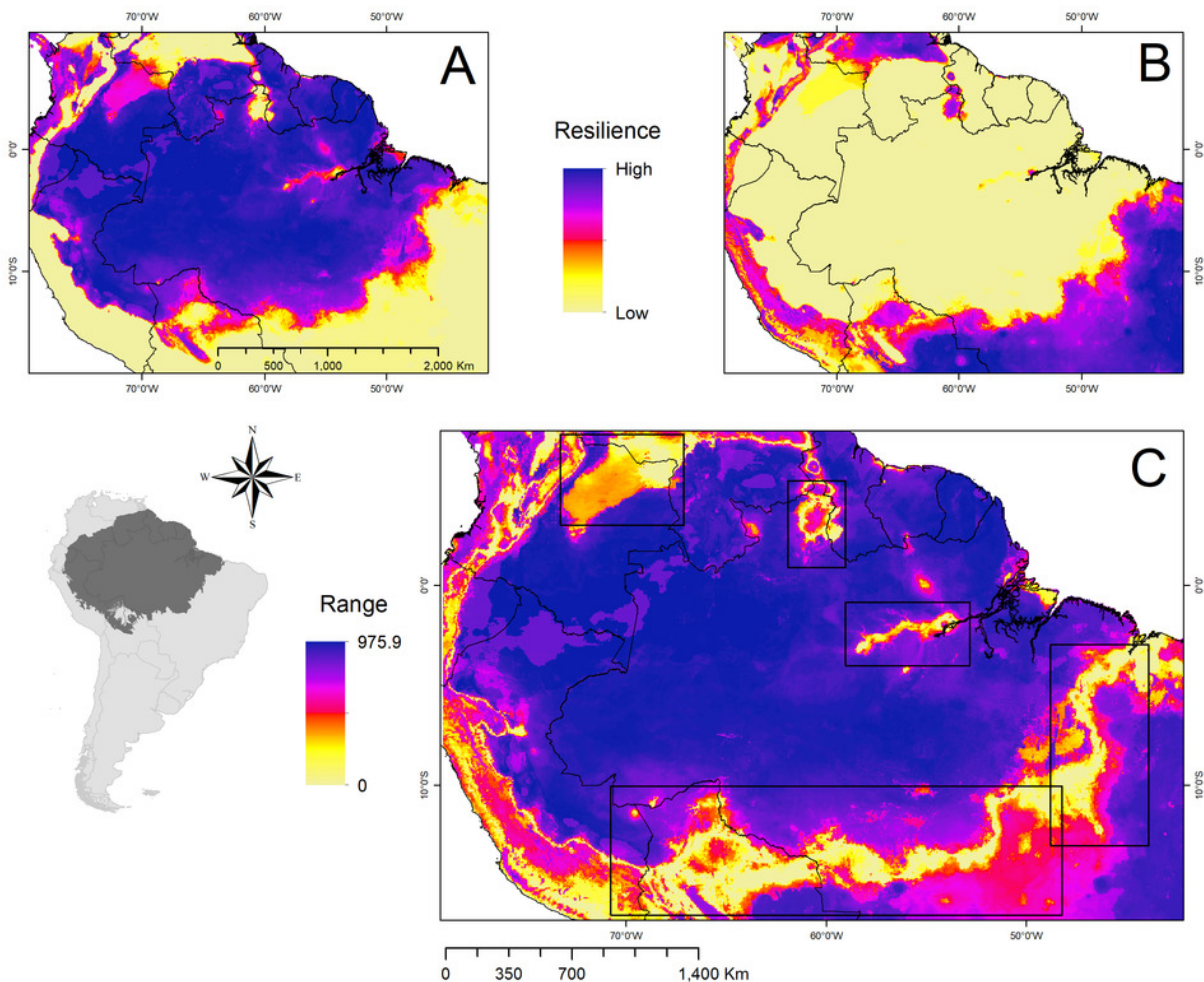


Figure 2

Critical resilience thresholds and the bistable ecotonal zone.

Under high resilience values (≥ 704) dominance of forests (green balls), while in low values (≤ 448) savannas stand out (purple balls). Under an intermediate zone of the resilience gradient (green-moss polygon), there is a balance of the observed proportions of forest and savanna, indicating an area of bistability. This transition zone should play a vital role in the mediation of stable state change events between forest and savanna.

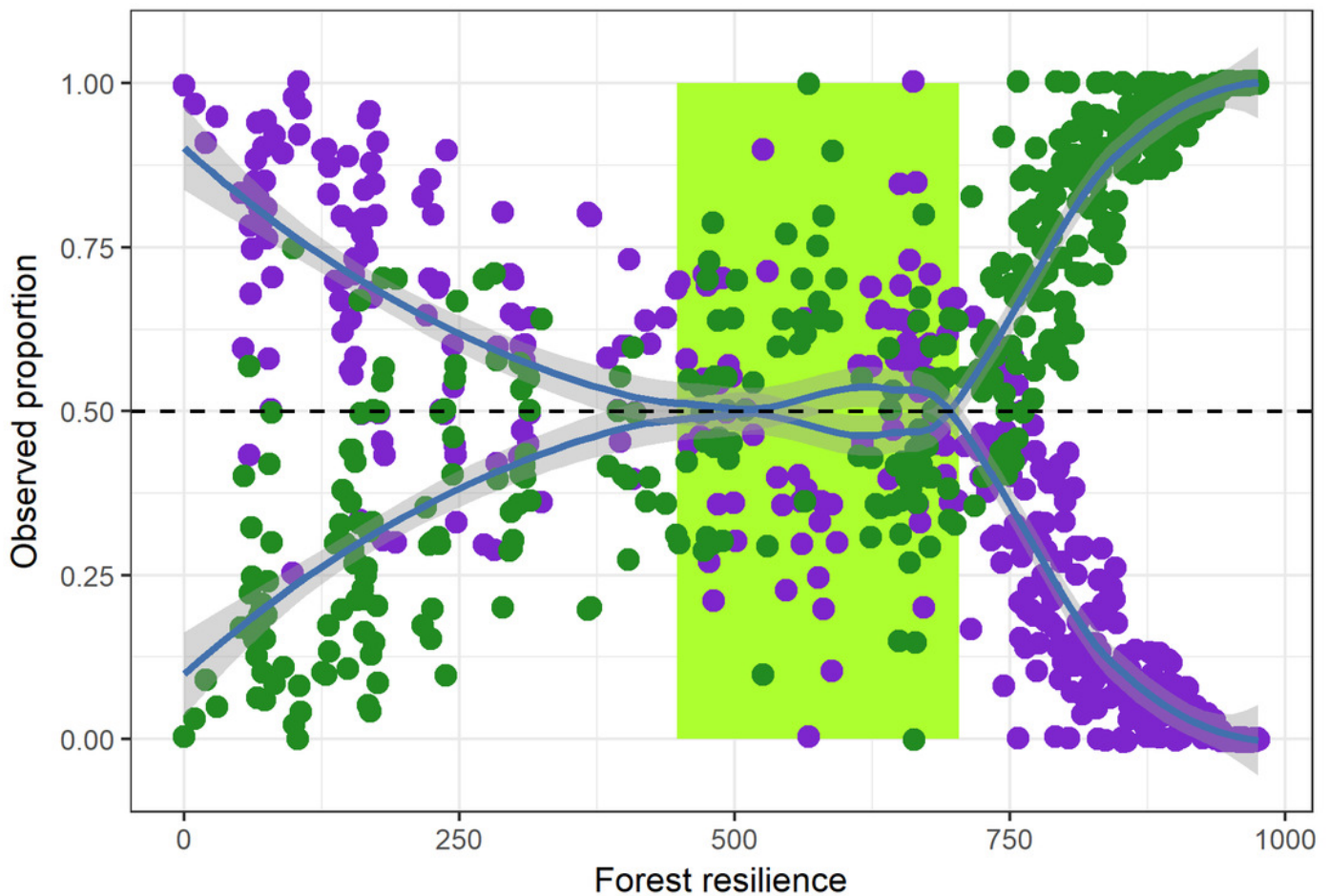


Figure 3

The propensity for catastrophic transition regimes under bidimensional climate space.

In (A) on the X-axis is the average annual temperature gradient (AAT) and on the Y-axis the annual cumulative precipitation (ACP). In (B) on the X-axis is the annual range of temperature (ART) and on the Y-axis is the seasonal precipitation coefficient (PSC). In all, we used $n=1805$ observations.

